# Spatiotemporal analysis of deforestation patterns and drivers reveals emergent threats to tropical forest landscapes

Jamaludin, Johanness

2022-05-01

Jamaludin , J , De Alban , J D T , Carrasco , L R & Webb , E L 2022 , ' Spatiotemporal analysis of deforestation patterns and drivers reveals emergent threats to tropical forest landscapes ' , Environmental Research Letters , vol. 17 , no. 5 , 054046 . https://doi.org/10.1088/1748-9326/ac68fa

http://hdl.handle.net/10138/344588
https://doi.org/10.1088/1748-9326/ac68fa

ENVIRONMENTAL RESEARCH
LETTERS

LETTER • OPEN ACCESS

# Spatiotemporal analysis of deforestation patterns and drivers reveals emergent threats to tropical forest landscapes

ENVIRONMENTAL RESEARCH
LETTERS

LETTER

# Spatiotemporal analysis of deforestation patterns and drivers reveals emergent threats to tropical forest landscapes

**Johanness Jamaludin**[1,2,*], **Jose Don T De Alban**[1,3], **L Roman Carrasco**[1,3] and **Edward L Webb**[1,2,4,*]

[1] Department of Biological Sciences, National University of Singapore, 117558, Singapore
[2] Viikki Tropical Resources Institute, Department of Forest Sciences, University of Helsinki, Latokartanonkaari 7, Helsinki, 00790, Finland
[3] Centre for Nature-based Climate Solutions, Department of Biological Sciences, National University of Singapore, 117558, Singapore
[4] Helsinki Institute of Sustainability Science (HELSUS), Yliopistonkatu 3, Helsinki, 00100, Finland
[*] Authors to whom any correspondence should be addressed.

**E-mail:** johanness.jamaludin@gmail.com **and** edward.webb@helsinki.fi

**Keywords:** conservation, hot spot, forest frontier, land change, tree plantations, protected areas

Supplementary material for this article is available online

OPEN ACCESS

RECEIVED
4 February 2022

REVISED
12 April 2022

ACCEPTED FOR PUBLICATION
21 April 2022

PUBLISHED
10 May 2022



## Abstract

As deforestation breaches into new tropical frontiers, proactive conservation strategies require a trifecta of information on where deforestation is accelerating (emergent), how drivers of deforestation vary spatiotemporally, and where to focus limited conservation resources in protecting the most integral yet threatened forested landscapes. Here we introduce Emergent Threat Analysis, a process integrating Emerging Hot Spot Analysis of deforestation, visual classification of deforestation outcomes over time, and spatial quantification of contemporary forest condition. We applied Emergent Threat Analysis to tropical Southeast Asia, a global epicentre of biodiversity threatened by deforestation. We found that emergent hot spots (EHS)—a subset of hot spots characterized by strong, recent, and clustered patterns of deforestation—accounted for 26.1% of total forest loss from 1992 to 2018, with deforestation within EHS proceeding at 2.5 times the regional rate of gross loss. Oil palm and rubber plantation expansion were the principal drivers of deforestation within EHS of insular and mainland SE Asia, respectively. Over the study period, oil palm shifted in importance from Sumatra and Sarawak to Papua and Kalimantan, whereas rubber became prominent in Cambodia and Tanintharyi from 2006 to 2015. As of 2019, more than 170 000 km$^2$ of SE Asia's remaining forest occurred within EHS, of which 21.7% was protected. High and medium-integrity forest constituted 19.2% and 49.1% of remaining EHS forest, respectively, but of these, 35.0% of high-integrity and 23.9% of medium-integrity EHS forest were protected. Because we anticipate that tree plantation expansion will continue to drive deforestation in SE Asia, significantly heightened protection is needed to secure the long-term preservation of high and medium-integrity forest, especially in highly contested forest frontier regions. Finally, as a flexible, integrated process, Emergent Threat Analysis is applicable to deforestation fronts across the global tropics.

## 1. Introduction

Deforestation is the most pervasive, imminent, existential threat to tropical forests worldwide; it results in a myriad of negative environmental outcomes including biodiversity loss, ecosystem service degradation, greenhouse gas emissions, and climate change (Gibbs and Herold 2007, Baccini *et al* 2012, Lawrence and Vandecar 2015, Giam 2017). In response, national policies along with international coalitions, treaties, and campaigns have evolved with the objectives of halting and reversing deforestation trends (IUCN, UNEP, and WCMC 2021, NYDF Assessment Partners 2021). The success of these campaigns is contingent in part, on the capacity to measure and track progress towards achieving deforestation reduction goals, which highlights an increasing need to leverage geospatial approaches to efficiently and effectively monitor, evaluate, and report deforestation trends at multiple scales. Even more pressing is the need to

know where deforestation threats to tropical forest frontiers are accelerating, what the drivers of deforestation are and how they vary across space and time, and where research, policy, and conservation interventions should proactively target to mitigate those new threats.

Numerous studies have quantitatively analysed the spatiotemporal variation in deforestation patterns across the tropics (Hansen *et al* 2010, 2013, Achard *et al* 2014, Nowosad *et al* 2019, to name a few); however, owing to the historical nature of geospatial data, they are typically retrospective in scope. While useful in deepening our understanding of landscape change processes, reliance on these analyses can render conservation science, policy, and intervention reactive to rapidly emerging trends. Significant efforts have been made to make geospatial data contemporaneous with deforestation occurrence (Hansen *et al* 2016, Reiche *et al* 2021); nevertheless, tools are urgently needed to identify emerging frontiers of deforestation so that proactive policy and intervention strategies can be developed. One such tool is Emerging Hot Spot Analysis (Harris *et al* 2017), a method that integrates spatial statistics and trend analysis to identify areas of recent and accelerating deforestation concern (which we refer to as 'emergent hot spots').

Far from being a homogeneous process, deforestation results from complex interactions of proximate and underlying drivers that vary considerably across spatial, temporal, and institutional scales (Geist and Lambin 2002, Bürgi *et al* 2005, Hersperger *et al* 2010, Hosonuma *et al* 2012, Lim *et al* 2017, De Alban *et al* 2020, Verma *et al* 2021). This is particularly true for dynamic deforestation environments such as emergent hot spots (EHS), which are likely to be subjected to rapidly changing deforestation drivers (Ramankutty and Coomes 2016, De Alban *et al* 2019). To respond to these dynamic threats, precise spatiotemporal attribution of proximate deforestation drivers is needed, which can be further linked to underlying drivers of deforestation and translated into targeted policy responses or interventions (Finer *et al* 2018). Indeed, although land cover data sets have greatly improved in temporal resolution, they remain unable to offer the same level of land use and land cover discrimination as very high-resolution (VHR) satellite imagery, which can be visually classified with high accuracy and efficiency, and at increasingly reduced barriers to availability and accessibility (Schepaschenko *et al* 2019).

Besides information on emergent trends and drivers of deforestation, conservation intervention must also strategically prioritize efforts and resources to where they are most needed. For example, the expansion of protected areas has been—and is expected to remain—the gold standard for conservation (Dudley and Phillips 2006, Maxwell *et al* 2020). Moreover, conservation organizations require enhanced information on where integral, yet threatened landscapes are, to justify directing limited conservation funding. To effectively safeguard biodiversity in landscapes facing emergent patterns and drivers of deforestation, conservation deployment requires a spatially informed understanding on contemporary forest health/condition, and its contribution to ecosystem function (Dinerstein *et al* 2017). This can be combined with information on existing levels of protection (Grantham *et al* 2020), which can then guide conservation planning to focus on the most threatened, high-value landscapes in a more proactive, rather than reactive, manner.

Here we introduce the Emergent Threat Analysis, which we define as the combined process of quantifying EHS of deforestation, precisely attributing the spatiotemporal drivers of deforestation, and identifying the most threatened high-conservation-value forests within those EHS. Emergent Threat Analysis differs from previous approaches to studying deforestation by virtue of its novel combination of methods that have all been utilized independently (Harris *et al* 2017, Grantham *et al* 2020), but which have yet to be fully integrated with the purpose of using dense, historical geospatial information to indicate priority regions for proactive and enhanced research, policy, and conservation attention.

Emergent Threat Analysis is critically needed in Southeast Asia, a region where globally important forests for biodiversity and carbon sequestration (Myers *et al* 2000, Sodhi *et al* 2004, Mitchard 2018) continue to face an emergent deforestation threat (Feng *et al* 2021, Hoang and Kanemoto 2021); the region is also where the highest rates of tropical deforestation have occurred in the past four decades (Miettinen *et al* 2011, Hansen *et al* 2013, Stibig *et al* 2014). Deforestation in SE Asia is driven primarily by agricultural expansion (Lepers *et al* 2005, Rudel *et al* 2009, Stibig *et al* 2014), with commodity-driven deforestation in the region outpacing all others worldwide from 2000 to 2015 (Curtis *et al* 2018). Indeed, SE Asia now accounts for the vast majority of global production of palm oil and natural rubber (Kenney-Lazar and Ishikawa 2019), two commodities that have been central in shaping regional and global agrarian economies. In addition to agriculture, deforestation in SE Asia is attributable to a wide range of spatiotemporally variable drivers that include logging, mining, aquaculture, and urbanization (Richards and Friess 2016, Hughes 2017, Lim *et al* 2017, Prescott *et al* 2017, De Alban *et al* 2020, Jayathilake *et al* 2020).

In this study we apply Emergent Threat Analysis across the entire region of SE Asia. First, we identify and quantify EHS of deforestation, which we contextualize using annual, historical patterns of deforestation from 1992 to 2018. Second, we characterize how land cover outcomes of deforestation within EHS have changed over time, to implicate the spatiotemporal dynamics of deforestation drivers.

Third, we combined the EHS analysis with forest landscape integrity to highlight conservation priorities and opportunities in the most threatened forest frontiers.

## 2. Methods

### 2.1. Quantifying dynamics of forest cover and change

Our analyses used the 1992–2018 European Space Agency (ESA) 300-m annual land cover dataset. We used this data because its long temporal domain was favourable for long-term trend analyses of forest change dynamics (De Alban *et al* 2019, Mousivand and Arsanjani 2019), and because it allowed us to incorporate pre-2000 deforestation data, which represented a period of intense deforestation in many parts of SE Asia. We projected the ESA data to the Equal-Area Scalable Earth Grid-2.0 cylindrical equal-area projection, which maximally preserved areal attributes over large geographical extents (Brodzik *et al* 2012).

To quantify forest change, we reclassified the ESA data into binary maps of forest and non-forest. Using the Intergovernmental Panel on Climate Change categorization in the ESA classification scheme (ESA 2017), we aggregated the eight ESA forest categories (broadleaved evergreen, broadleaved deciduous, needleleaved evergreen, needleleaved deciduous, mixed broadleaved/needleleaved, mosaic tree/shrub, flooded freshwater/brackish, and flooded saline water) into a single 'Forest' category, and reclassified all others as 'Non-forest'. We then differenced pairs of binary forest/non-forest maps using Google Earth Engine to create 26 interannual forest change maps, and one for the entire 1992–2018 interval (i.e. differencing 1992 and 2018). The 1992–2018 forest change map was used to quantify overall forest change statistics over the 26-year period, while the interannual change maps were used to construct the annual time series of net and gross forest change, and to quantify the amount of loss that occurred within EHS.

We then tessellated the SE Asian region into 5-km circumradius hexagons to aggregate data on interannual gross forest loss (supplementary methods (SM) 1.2, 1.3, and figure S1 available online at stacks.iop.org/ERL/17/054046/mmedia). Aggregating pixel data into hexagons facilitated spatial analysis of forest cover and change. Further, the hexagons provided spatially equivalent analytical units as required for hot spot analysis (next section). Given the area of each hexagon (~65 $km^2$), they are referred to as 'landscapes' in the results (section 3) (Nowosad *et al* 2019).

To investigate the spatial relationships between initial forest cover and gross deforestation across SE Asia for the 26-year period, we created a bivariate classification of initial (1992) forest cover and 1992–2018 gross loss. Initial forest cover was calculated as the percentage of hexagon area while gross loss was calculated as the percentage of initial forest cover. Based on the respective data distributions for each metric, initial forest cover was binned into marginally (<30%), moderately (30%–72%), and heavily (>72%) forested hexagons, whereas gross loss area was binned into weak (<10%), moderate (10%–42%), and intense (>42%) deforestation (SM 1.1). Binning was performed in R using the *classInt* package (Bivand *et al* 2020).

Quantification and data visualization was performed in R (R Core Team 2020) using the *raster, sf, tidyr, dplyr, landscapemetrics*, and *ggplot2* packages (Hesselbarth *et al* 2019, Hijmans *et al* 2021, Pebesma *et al* 2021, Wickham 2021, Wickham *et al* 2021a, 2021b), and cartography was done in QGIS (QGIS Development Team 2021).

### 2.2. Identifying EHS of deforestation

We identified and quantified EHS deforestation using the Emerging Hot Spot Analysis (Harris *et al* 2017, hereafter referred to as Hot Spot Analysis). Hot spots were identified by analysing the amount of forest loss in a hexagon neighbourhood in relation to the total amount of loss within a predetermined landscape, using Getis-Ord $G_i^*$ to test for spatial clustering of deforestation within a hexagon neighbourhood, and the Mann-Kendall trend test to evaluate for temporal trends of deforestation (Mann 1945, Kendall and Gibbons 1990, Getis and Ord 1992, Harris *et al* 2017, ArcGIS 2021).

Following Harris *et al* (2017), we analysed SE Asia by subregions in order to identify hot spots that were likely driven by and related to subregion-specific social, political, and economic contexts. We defined subregions using national-level boundaries from the Global Administrative Areas data, except for the following Indonesian island subregions: Sumatra, Kalimantan, Java and Nusa Tenggara, Sulawesi and Maluku, and Papua (adapted from Margono *et al* 2014). Singapore, Brunei, and Timor Leste were subsumed within their neighbouring regions owing to their small land areas. In total, there were 12 subregions for Hot Spot Analysis. For each subregion, we aggregated pixel-scale information from the forest change maps into the hexagonal grid, resulting in a spatially explicit, annual time series of subregional deforestation density from 1992 to 2018 (SM 1.4). We then performed Hot Spot Analysis for each subregion and masked out areas of forest/non-forest persistence (table S1, and SM 1.5).

Hot Spot Analysis categorizes deforestation patterns per hexagon into hot spots (eight types), cold spots (eight types), or without a pattern (ArcGIS 2021). As our emphasis was on areas of recent and accelerating deforestation, we focused on consecutive, intensifying, and persistent hot spots. Consecutive hot spots meant that deforestation trends developed over an uninterrupted series of time intervals (ArcGIS 2021). Persistent hot spots

were identified when deforestation was consistently clustered over time (ArcGIS 2021). Intensifying hot spots were similar to persistent hot spots, but in addition, they were identified when the intensity of deforestation clustering increased over time (ArcGIS 2021). We consolidated consecutive, intensifying, and persistent hot spots into EHS because these three hot spot types exhibited (1) strong patterns of clustered deforestation over time, and (2) were identified in the final time step, thereby including an element of recency (table S2 and figure S2). The other hot spot types (i.e. diminishing, historical, oscillating, sporadic, and new) did not reflect strong, recent, and developing trends of clustered forest loss, and thus did not represent as much of a growing deforestation threat (SM 1.6). We then merged the 12 subregional Hot Spot Analysis outputs together to create the EHS map for SE Asia, which was used for subsequent analyses.

### 2.3. Classifying land cover outcomes of hot spot deforestation

We conducted a sample-based visual assessment of land cover changes associated with hot spot deforestation. Using a stratified random sampling approach, we selected interannual forest loss pixels within each EHS region, and grouped them into three-year intervals (e.g. 2000–2003, 2003–2006, etc; the 2015–2017 period only contained two interannual intervals). Distance between selected pixels was $\geqslant$5 km to ensure independence. The initial sample count of 1146 was distributed across subregions in proportion to the total amount of interannual forest loss from 2000 to 2017; no samples were allocated in the EHS of Java, Nusa Tenggara, Timor Leste, and the Philippines, each of which accounted for $\sim$1.0% of total loss during this period (table S3). Samples were filtered to include those with sufficient, interpretable images to confidently ascertain both (1) the deforestation event (false positives were rejected) and (2) the resultant land cover following deforestation. After filtering, 571 samples were used in the visual assessment of land cover outcomes (figure S3).

We classified 14 deforestation land cover outcomes under general themes of tree plantations, farming systems, degraded landscapes, and other land (figure S4). Tree plantations consisted of oil palm, rubber, pulpwood, cashew, and coconut. Farming systems included rice cultivation, mixed farming/homegardens, and shifting cultivation. Degraded landscapes consisted of shrub/grassland and bare ground that could be intermediate or permanent; a special category of this was degraded forest, where reductions in forest cover were observed over time without evidence of deforestation. Other land included built up areas, artificial water bodies, and mining.

We set five years post-deforestation as the window to classify land cover outcomes of deforestation because our preliminary assessment revealed that oil palm, rubber, and pulpwood plantations were identifiable within that time frame if the land was immediately cultivated. In this case, the immediate post-deforestation outcome was assumed to be the deforestation driver because the conversion was likely driven by an intended land use outcome. In some cases, however, the conversion of forest into a long-term land cover outcome may be delayed, inducing a transitory intermediate land cover in the process. To include these transitions, we also evaluated the land cover of all samples in 2021; however, we did not assess 2021 land cover for samples deforested in 2017 because the initial and final outcomes would have been synonymous.

Classification of land cover outcomes was performed using Collect Earth (Bey *et al* 2016), in which visual interpretation of VHR imagery in Google Earth was the primary analysis, supplemented when necessary by annual Landsat and Sentinel imagery in Google Earth Engine. Infrared false colour composites from Landsat and Sentinel offered contextual information regarding the evolution of land cover over time and allowed us to discriminate between rubber and pulpwood plantations, which have similar canopy morphologies. Data entry was achieved through a customized survey form in Open Foris Collect (https://openforis.org/tools/collect/). Land cover outcomes were quantified as a percentage of subregional samples in each three-year interval.

### 2.4. Evaluating contemporary forest integrity and protection

We leveraged the 2019 Forest Landscape Integrity Index (FLII) to quantify the integrity of naturally occurring or regenerating forest that remained in EHS. FLII delivered 300-m information on forest integrity that was calculated as a function of forest extent, human pressure, and landscape connectivity (Grantham *et al* 2020). Before integrating the FLII data, we used the 2018 ESA forest cover map as a mask to exclude tree plantations and urban greenery from that dataset (SM 1.7). We then discretized the continuous FLII data into high, medium, and low integrity, using the thresholds defined by Grantham *et al* (2020). High-integrity forest (FLII $\geqslant$ 9.6) represented core areas that were largely unmodified and with ecosystems functioning at near-natural levels. Medium-integrity forest (FLII $>$ 6.0 and $<$ 9.6) had sustained higher degrees of modification, resulting in lower provisioning of ecosystem services. Low-integrity forest (FLII $\leqslant$ 6.0) referred to areas that were extensively modified, fragmented, and were expected to have weak contributions to ecosystem function. Given that the FLII categories carry significant ecological relevance, we were able to identify the areas of highest conservation priority in landscapes threatened by deforestation.

We then quantified protected area coverage within EHS and stratified this analysis by forest integrity to identify where current gaps in the protection of threatened high and medium-integrity forest existed. Protected area data were primarily sourced from the International Union for Conservation of Nature World Database on Protected Areas (IUCN, UNEP-WCMC 2020), and the Wildlife Conservation Society Myanmar. We dissolved the protected area data into a single layer to prevent double-counting (UNEP-WCMC 2015), and clipped it to each EHS region. By spatially joining protected area and forest integrity data within EHS, we were able to quantify the amount of protected and unprotected forest that was threatened with emergent deforestation.

## 3. Results

### 3.1. Spatiotemporal dynamics of deforestation, 1992–2018

In 1992, forest cover in SE Asia was 2343 773 $km^2$, of which 65.7% was in insular SE Asia (table 1). From 1992 to 2018, gross forest loss was 219 833 $km^2$, balanced by a gain of 143 215 $km^2$ for a net loss of 76 618 $km^2$ ($-0.13\%$ $yr^{-1}$, table 1). Insular SE Asia accounted for 98.7% of total net loss and 65.2% of total forest change (gross losses + gross gains) (table 1). Thus, total forest change in insular and mainland SE Asia was proportional to the amount of 1992 forest cover, but net losses were almost all contained in insular SE Asia (figure S5). Cambodia was an outlier in mainland SE Asia, with annual net losses of $-0.60\%$, comprising a unique combination of high gross loss and almost no gross gain (table 1).

Interannual forest change varied considerably across the subregions, exhibiting six temporal trajectories (figure 1). Consistent net losses occurred for more than 80% of the time period in Sumatra, Kalimantan, East Malaysia, and Sulawesi and Maluku. Attenuating losses, which indicated reduced deforestation rates over time, occurred in Cambodia, Vietnam, and Singapore. Thailand exhibited a period of consistent net forest loss until 2003 followed by consistent net forest gain, i.e. a 'forest transition' *sensu* (Mather 1992). Oscillating patterns, which occurred when forest change cycled between periods of net losses and gains were observed in Papua, Brunei, and Laos. West Malaysia exhibited a short period of net gain that was succeeded by an uninterrupted period of net loss that spanned 75% of the time series. Finally, net gains for more than 60% of the time period were recorded in Myanmar, Java and Nusa Tenggara, Philippines, and Timor Leste.

Through bivariate mapping of forest cover in 1992 and gross forest losses for 1992–2018 (figure 2), we found that heavily forested landscapes (i.e. hexagons with > 72.0% forest cover) contained 70.3% of total forest cover in 1992 and accounted for 48.1% of gross losses (table S4). Moderately forested landscapes (i.e. hexagons with 30.0%–72.0% forest cover) were targeted for deforestation, as evidenced by the fact that they contained 24.5% of initial forest cover but accounted for 42.4% of gross loss (table S4). Heavily and moderately forested landscapes that experienced intense deforestation—defined as $\geqslant$ 42.0% reduction in initial cover—contained 7.0% of all SE Asia's forest in 1992 and accounted for 50.6% of gross loss from 1992 to 2018 (table S4). These were the areas where deforestation over the 26-year period was most concentrated; observed in Sumatra, Kalimantan, Sarawak, south Myanmar (i.e. Tanintharyi), Cambodia, and central Vietnam (figure 2).

### 3.2. EHS of deforestation

Gross forest loss occurred in a diverse mosaic of hot and cold spots that indicated a complex mélange of deforestation dynamics across SE Asia (figures S6 and S7). Interannual gross forest loss from 1992 to 2018 totalled 233 950 $km^2$ (table S5), of which EHS accounted for 61 140 $km^2$, i.e. 26.1% (table 2). EHS deforestation led to a 24.0% gross reduction in 1992 forest cover, with gross losses occurring at a rate of 0.92% $yr^{-1}$, which was 2.5 times the regional rate of gross loss (0.36% $yr^{-1}$, table 1).

EHS deforestation impacted insular SE Asia proportionately more than mainland SE Asia: whereas 63.9% of EHS forest cover was insular (consistent with 65.6% of all of SE Asia's forest being insular), it accounted for 71.9% of EHS deforestation (table 2). The greatest gross decline was 48.9%, in the Sumatran EHS, while other EHS experiencing gross declines greater than 20% included Kalimantan (36.2%), Malaysia (32.8%), Cambodia (29.6%), Vietnam (23.4%), and Myanmar (20.5%). Altogether, these six regions accounted for 84.9% of total EHS deforestation in SE Asia (table 2).

### 3.3. Land cover outcomes of deforestation within EHS

The most prevalent land cover outcome of EHS deforestation was tree plantations, which comprised 45.7% of initial and 62.2% of final outcomes (table 3). Tree plantations, mostly in the form of oil palm plantations, dominated in all insular EHS (53.2% $\rightarrow$ 67.4%, initial to final, table 3) except Sulawesi, which was dominated by conversions into shrub/grassland (50.0%, table S6). Over time, the importance of oil palm as a deforestation outcome declined in Sumatra and Sarawak, whereas it increasingly drove deforestation in Papua and Kalimantan (figure 3). In mainland SE Asia, tree plantation outcomes had an initial occurrence rate of 21.5%, but this increased to 45.2% by 2021 (table 3). Rubber plantations were the primary tree plantation type across mainland EHS (11.1% $\rightarrow$ 23.0%, table 3). They were most prominent in EHS of Cambodia and Tanintharyi, predominating from 2006 to 2015 (figure 3) when rubber prices were increasing (figure S8).

**Table 1.** Forest cover and change statistics for SE Asia, 1992–2018. Losses and gains are reported as gross statistics. Annual change rate is the percentage of 1992 forest that underwent change by 2018, divided by 26 years. Areas were calculated using projected ESA data.

| | | Forest area ($km^2$) | | Forest change ($km^2$) | | | Annual change rate (%) | | |
|---|---|---|---|---|---|---|---|---|---|
| Region | Area ($km^2$) | 1992 | 2018 | Loss | Gain | Net | Loss | Gain | Net |
| *Insular SE Asia* | | | | | | | | | |
| Kalimantan | 533 937 | 367 983 | 333 019 | 49 977 | 15 013 | −34 964 | 0.52 | 0.16 | −0.37 |
| Sumatra | 475 383 | 231 265 | 197 146 | 48 485 | 14 366 | −34 118 | 0.81 | 0.24 | −0.57 |
| East Malaysia | 197 607 | 156 833 | 145 925 | 20 810 | 9903 | −10 907 | 0.51 | 0.24 | −0.27 |
| Sulawesi and Maluku | 264 240 | 187 858 | 184 016 | 11 585 | 7743 | −3842 | 0.24 | 0.16 | −0.08 |
| West Malaysia | 131 776 | 66 649 | 64 420 | 8449 | 6221 | −2228 | 0.49 | 0.36 | −0.13 |
| Papua | 412 305 | 373 968 | 372 331 | 5629 | 3992 | −1637 | 0.06 | 0.04 | −0.02 |
| Singapore | 697 | 128 | 90 | 53 | 15 | −38 | 1.60 | 0.46 | −1.14 |
| Brunei | 5778 | 4868 | 4952 | 79 | 164 | 85 | 0.06 | 0.13 | 0.07 |
| Timor Leste | 14 915 | 2055 | 2255 | 87 | 288 | 201 | 0.16 | 0.54 | 0.38 |
| Philippines | 295 857 | 100 877 | 103 717 | 8679 | 11 519 | 2840 | 0.33 | 0.44 | 0.11 |
| Java and Nusa Tenggara | 204 379 | 46 723 | 55 688 | 2344 | 11 310 | 8965 | 0.19 | 0.93 | 0.74 |
| **Subtotal** | **2536 875** | **1539 206** | **1463 562** | **156 177** | **80 533** | **−75 644** | **0.39** | **0.20** | **−0.19** |
| *Mainland SE Asia* | | | | | | | | | |
| Cambodia | 181 360 | 99 459 | 83 862 | 16 402 | 804 | −15 598 | 0.63 | 0.03 | −0.60 |
| Vietnam | 329 276 | 127 329 | 116 555 | 16 631 | 5857 | −10 774 | 0.50 | 0.18 | −0.33 |
| Thailand | 514 055 | 129 553 | 131 460 | 7222 | 9130 | 1908 | 0.21 | 0.27 | 0.06 |
| Laos | 230 002 | 125 365 | 128 993 | 7073 | 10 702 | 3628 | 0.22 | 0.33 | 0.11 |
| Myanmar | 669 297 | 322 861 | 342 723 | 16 327 | 36 189 | 19 862 | 0.19 | 0.43 | 0.24 |
| **Subtotal** | **1923 989** | **804 567** | **803 592** | **63 655** | **62 681** | **−974** | **0.30** | **0.30** | **0.00** |
| **Total SE Asia** | **4460 865** | **2343 773** | **2267 154** | **219 833** | **143 215** | **−76 618** | **0.36** | **0.24** | **−0.13** |

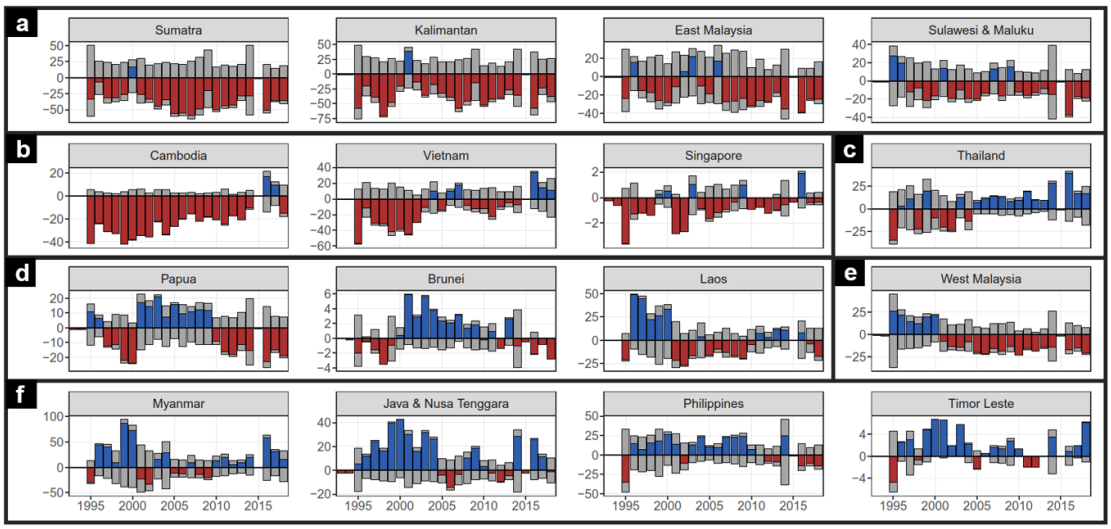


**Figure 1.** Interannual patterns of net and gross forest change in subregions of SE Asia. Gross (grey) and net (blue for gain; red for loss) forest change, with $Y$-axis representing $\sqrt{\text{Forest change area (km}^2\text{)}}$ over 26 interannual time intervals for the subregions of SE Asia. Trends were characterized into six temporal patterns; (a) consistent losses, (b) attenuating losses, (c) forest transition, (d) oscillating, (e) short period of gain followed by consecutive losses, and (f) consistent gains.

Degraded landscapes accounted for 44.0% of all initial outcomes and was predominately shrub/-grassland in all EHS regions (except Papua, table S6), followed by bare ground and degraded forest (table 3). However, 49.0% of degraded landscapes were subsequently converted to another land cover (figure 4), reducing its importance to 27.7% (table 3). Such conversions from intermediate to final outcomes generally followed the subregional trends of direct deforestation, i.e. towards oil palm and rubber plantations (figure 4, tables S7 and S8). A notable exception was cashew, in which a majority of outcomes arose from six types of intermediate transitions in mainland EHS (table S8), reflecting its growing prominence amongst other land cover outcomes.

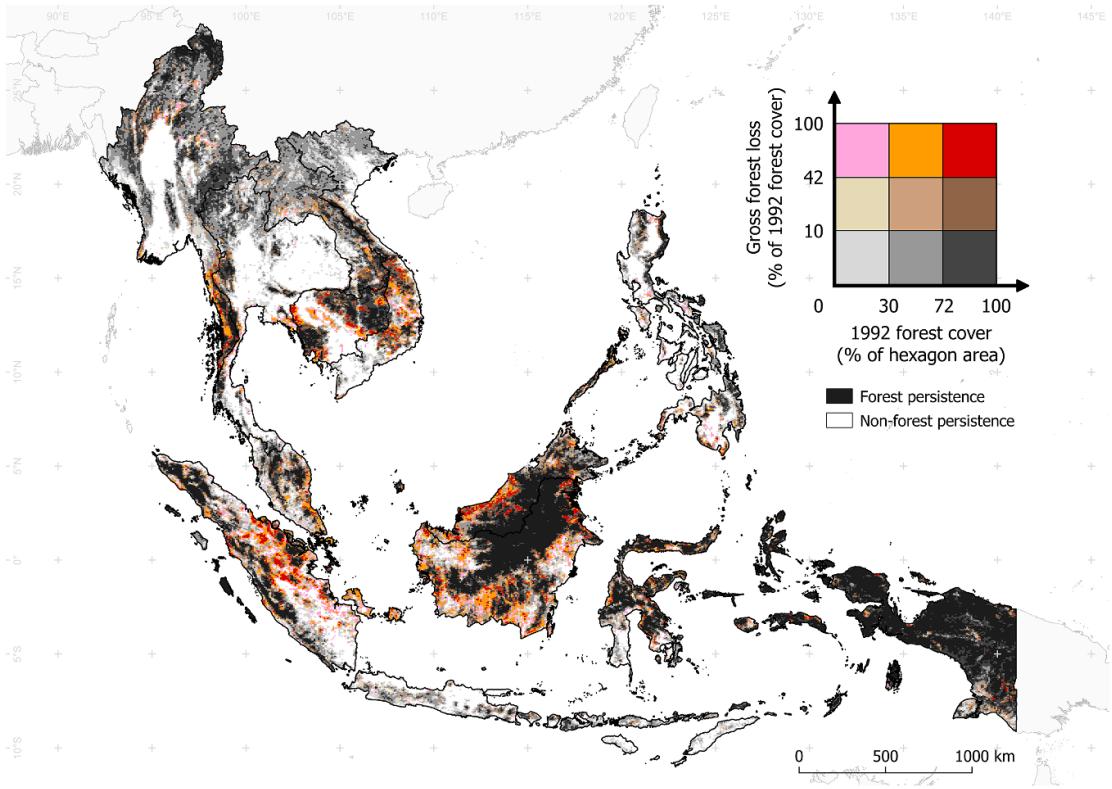


**Figure 2.** Forest cover in 1992 and gross forest loss from 1992 to 2018, where each map unit is a 5-km circumradius hexagon (~65 km$^2$). *Y*-axis breaks were defined using a head-tails (heavy-skew) method, while *X*-axis breaks were defined using a natural breaks (jenks) method to suit their respective data distributions.

**Table 2.** Forest cover and interannual gross loss in emergent hot spots (EHS) of SE Asia. EHS area refers to the geographical area covered by EHS. Percentage of gross loss was calculated with respect to 1992 cover. The following values are appended here to support interpretation: (a) total interannual gross loss in SE Asia was 233 950 km$^2$, and (b) total 2018 forest area in SE Asia was 2267 154 km$^2$. Note that this table does not include gross gains or net forest change. Areas were calculated using projected data.

| | | Forest area (km$^2$) | | Gross loss, 92–18 | |
|---|---|---|---|---|---|
| Region | EHS area (km$^2$) | 1992 | 2018 | km$^2$ | % |
| *Insular SE Asia* | | | | | |
| Kalimantan | 27 133 | 16 358 | 11 750 | 5930 | 36.2 |
| Sumatra | 79 886 | 45 166 | 24 805 | 22 082 | 48.9 |
| Malaysia | 44 629 | 32 462 | 24 123 | 10 650 | 32.8 |
| Sulawesi | 31 478 | 25 223 | 23 180 | 2528 | 10.0 |
| Papua | 40 436 | 32 947 | 31 920 | 2043 | 6.2 |
| Java and Nusa Tenggara | 30 811 | 9470 | 11 228 | 575 | 6.1 |
| Philippines | 3236 | 1208 | 1125 | 151 | 12.5 |
| **Subtotal** | **257 609** | **162 835** | **128 132** | **43 959** | **27.0** |
| *Mainland SE Asia* | | | | | |
| Cambodia | 11 110 | 8224 | 5724 | 2433 | 29.6 |
| Vietnam | 37 604 | 29 493 | 22 851 | 6895 | 23.4 |
| Thailand | 18 939 | 12 992 | 11 092 | 1379 | 10.6 |
| Laos | 29 525 | 22 214 | 20 628 | 2527 | 11.4 |
| Myanmar | 22 257 | 19 238 | 15 051 | 3947 | 20.5 |
| **Subtotal** | **119 434** | **92 162** | **75 346** | **17 181** | **18.6** |
| **Total** | **377 043** | **254 997** | **203 478** | **61 140** | **24.0** |

Of the farming-related outcomes, shifting cultivation made only a minor contribution to EHS deforestation (table 3), and was most prominent in southern Laos (table S6). Further, of all initial outcomes identified as shifting cultivation, 55.6% were converted into rubber (33.3%) and cashew (11.1%) plantations, and mixed farming/homegardens (11.1%), while the remainder were identified

**Table 3.** Percentage of initial and final land cover outcomes of deforestation in insular and mainland SE Asia. Initial outcomes refer to the land cover at five years post-deforestation, while final outcomes refer the 2021 land cover. '*n*' denotes the number of samples.

| | Insular ($n = 436$) | | Mainland ($n = 135$) | | All ($n = 571$) | |
|---|---|---|---|---|---|---|
| Land cover outcome | Initial | Final | Initial | Final | Initial | Final |
| *Tree plantation* | | | | | | |
| Oil palm | 46.1 | 60.3 | 5.2 | 8.1 | 36.4 | 48.0 |
| Rubber | 1.1 | 0.9 | 11.1 | 23.0 | 3.5 | 6.1 |
| Pulpwood | 4.4 | 5.3 | — | — | 3.3 | 4.0 |
| Cashew | — | — | 4.4 | 12.6 | 1.1 | 3.0 |
| Coconut | 0.5 | 0.5 | — | — | 0.4 | 0.4 |
| Immature tree crop | 1.1 | 0.5 | 0.7 | 1.5 | 1.1 | 0.7 |
| **Subtotal** | **53.2** | **67.4** | **21.5** | **45.2** | **45.7** | **62.2** |
| *Farming* | | | | | | |
| Rice cultivation | — | — | 2.2 | 2.2 | 0.5 | 0.5 |
| Mixed farming | 2.8 | 2.5 | 8.9 | 11.9 | 4.2 | 4.7 |
| Other crop | 0.5 | 0.5 | 0.7 | 4.4 | 0.5 | 1.4 |
| Shifting cultivation | 0.5 | 0.5 | 6.7 | 1.5 | 1.9 | 0.7 |
| **Subtotal** | **3.7** | **3.4** | **18.5** | **20.0** | **7.2** | **7.4** |
| *Degraded* | | | | | | |
| Shrub/grassland | 33.0 | 22.5 | 40.0 | 21.5 | 34.7 | 22.2 |
| Degraded forest | 3.0 | 1.6 | 6.7 | 3.0 | 3.9 | 1.9 |
| Bare ground | 3.9 | 2.3 | 10.4 | 7.4 | 5.4 | 3.5 |
| **Subtotal** | **39.9** | **26.4** | **57.0** | **31.9** | **44.0** | **27.7** |
| *Other* | | | | | | |
| Built up area | 0.9 | 0.5 | 0.7 | 0.7 | 0.9 | 0.5 |
| Mining | 2.1 | 2.1 | 1.5 | 1.5 | 1.9 | 1.9 |
| Water body | 0.2 | 0.2 | 0.7 | 0.7 | 0.4 | 0.4 |
| **Subtotal** | **3.2** | **2.8** | **3.0** | **3.0** | **3.2** | **2.8** |
| **Total percentage** | **100** | **100** | **100** | **100** | **100** | **100** |

as active swidden or shrub/grassland that arose from swidden abandonment or fallow.

### 3.4. Forest integrity and protection in EHS

As of 2018, EHS contained 9.0% of total remaining forest in SE Asia (table 2). Based on the FLII, 170 737 km$^2$ of forest remained within EHS, of which 64.4% occurred in insular SE Asia (table 4). Overall, 19.2% of remaining EHS forest in SE Asia exhibited high integrity, 49.1% medium integrity, and 31.7% low integrity; these percentages were similar for both insular and mainland EHS (table 4).

High-integrity forests comprised <10.0% of forest area in most EHS regions (table 4). Notable exceptions of EHS with substantial proportions of high-integrity forest were Papua (47.8%, 15 117 km$^2$), Sulawesi (20.6%, 4636 km$^2$), southern Myanmar (36.0%, 4319 km$^2$) and western Thailand (50.2%, 4191 km$^2$) (the latter two encompass the Dawna Tenasserim landscape, figure 5). A majority of the remaining EHS were dominated by medium-integrity forest, such as in central Sumatra, southern Laos, and central Vietnam (table 4); only a small proportion of high-integrity forest remained in these areas (figure 5).

As of 2019, protected areas covered 36 980 km$^2$ (21.7%) of remaining forest in EHS across SE Asia; they covered 35.0% of high-integrity forest, 23.9% of medium-integrity forest, and 10.1% of low-integrity forest (table 4). At the subregional level, however, protection status varied widely by forest integrity (figure 6). Protected areas covered >30% of EHS forest in Sumatra (30.2%), Myanmar (41.1%), Brunei (45.2%), Cambodia (46.6%), and Thailand (84.9%); however, only in Thailand and Myanmar did this represent more than 2000 km$^2$ of high-integrity forest (table 4).

The largest area of unprotected high-integrity forest was 14 045 km$^2$, in Papua's EHS where only 7.1% of high-integrity forest was protected (table 4). Other EHS with >1000 km$^2$ of unprotected high-integrity forest include Sulawesi, Laos, and Myanmar. Medium and low-integrity forest formed the bulk of unprotected forest (table 4), but the proportional contributions of these forest types varied considerably across EHS subregions (figure 6).

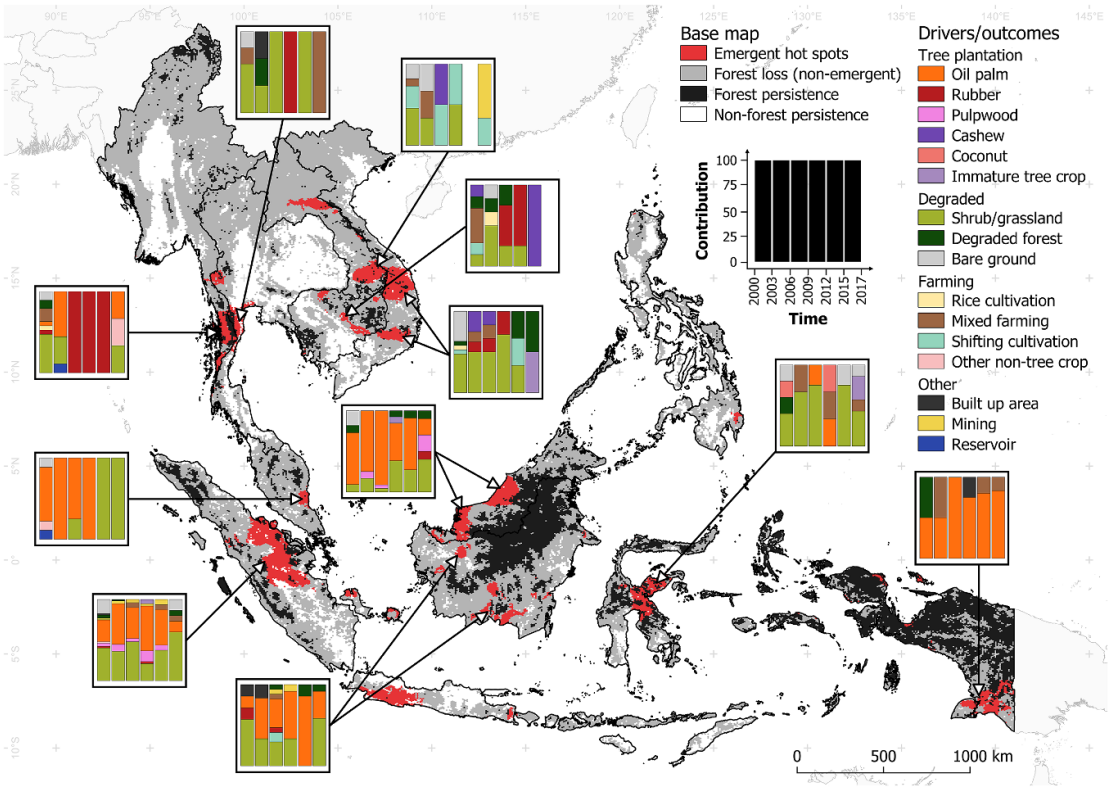


**Figure 3.** Initial land cover outcomes of deforestation in emergent hot spots, 2000–2017. Stacked bar plots reflect the per cent of each forest loss outcome in three-year intervals (bars) from 2000 to 2017, for 571 randomly selected forest loss samples. The absence of bars in 2012–2015 for Cambodia and 2015–2017 for Laos were because forest loss in each of the two regions accounted for only 0.1% of total interannual 2000–2017 loss in SE Asia.

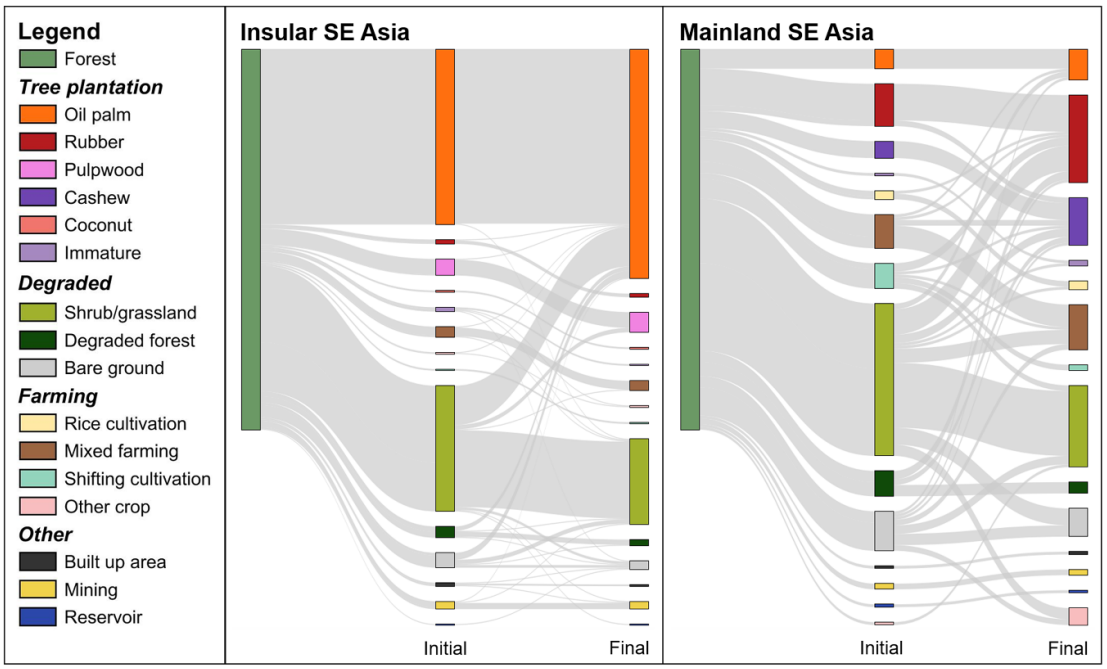


**Figure 4.** Land cover trajectories of deforestation in emergent hot spots of insular and mainland SE Asia. Sankey diagrams depict the initial (five-year post-deforestation) and final (2021) land cover outcomes of forest loss. In both insular and mainland SE Asia, degraded habitat served as a major intermediate land cover, prior to conversion to the final land cover outcome.

**Table 4.** Contemporary forest cover, integrity, and protected area (PA) coverage, in emergent hot spots (EHS) of SE Asia. High, med (medium), and low refer to the three categories of forest integrity. Here, EHS forest areas were calculated from the 2019 Forest Landscape Integrity Index data, and thus differ from the values reported in table 2, which used the 2018 ESA data.

| | | Forest integrity (%) | | | Within a PA (%) | | | Protected forest, all | | Unprotected forest ($km^2$) | | | |
|---|---|---|---|---|---|---|---|---|---|---|---|---|---|
| Region | EHS forest ($km^2$) | High | Med | Low | High | Med | Low | $km^2$ | % | High | Med | Low | All |
| *Insular SE Asia* | | | | | | | | | | | | | |
| Kalimantan | 9304 | 0.6 | 37.9 | 61.6 | 0.0 | 17.0 | 8.6 | 1092 | 11.7 | 54 | 2923 | 5235 | 8212 |
| Sumatra | 15 548 | 2.1 | 54.2 | 43.8 | 42.8 | 43.4 | 13.2 | 4697 | 30.2 | 183 | 4765 | 5902 | 10 851 |
| West Malaysia | 1437 | 0.1 | 42.1 | 57.7 | 49.5 | 17.6 | 2.1 | 125 | 8.7 | 1 | 499 | 812 | 1312 |
| East Malaysia | 17 193 | 3.5 | 37.3 | 59.2 | 81.9 | 7.3 | 1.9 | 1159 | 6.7 | 110 | 5941 | 9983 | 16 034 |
| Brunei | 102 | 0.0 | 96.1 | 3.9 | NA | 45.7 | 33.0 | 46 | 45.2 | NA | 53 | 3 | 56 |
| Sulawesi | 22 504 | 20.6 | 56.0 | 23.4 | 32.2 | 14.8 | 5.9 | 3664 | 16.3 | 3144 | 10 731 | 4966 | 18 840 |
| Papua | 31 625 | 47.8 | 43.8 | 8.4 | 7.1 | 6.5 | 1.6 | 2019 | 6.4 | 14 045 | 12 955 | 2606 | 29 606 |
| Java and Nusa Tenggara | 11 155 | 1.9 | 62.9 | 35.2 | 17.9 | 11.5 | 3.1 | 965 | 8.7 | 175 | 6212 | 3802 | 10 190 |
| Philippines | 1105 | 3.8 | 64.8 | 31.4 | 0.0 | 10.1 | 7.1 | 97 | 8.8 | 42 | 644 | 322 | 1008 |
| **Subtotal** | **109 973** | **19.1** | **48.4** | **32.5** | **15.4** | **16.0** | **5.9** | **13 865** | **12.6** | **17 753** | **44 723** | **33 632** | **96 108** |
| *Mainland SE Asia* | | | | | | | | | | | | | |
| Cambodia | 2422 | 2.0 | 24.1 | 73.9 | 100.0 | 85.1 | 32.6 | 1128 | 46.6 | 0 | 87 | 1207 | 1294 |
| Vietnam | 18 721 | 7.8 | 51.9 | 40.2 | 69.8 | 28.6 | 10.6 | 4604 | 24.6 | 443 | 6945 | 6729 | 14 117 |
| Thailand | 8348 | 50.2 | 39.0 | 10.9 | 97.0 | 85.9 | 25.9 | 7091 | 84.9 | 126 | 459 | 671 | 1257 |
| Laos | 19 275 | 8.9 | 58.6 | 32.5 | 35.8 | 30.5 | 20.8 | 5362 | 27.8 | 1103 | 7850 | 4960 | 13 913 |
| Myanmar | 11 998 | 36.0 | 47.9 | 16.2 | 56.9 | 35.5 | 22.5 | 4930 | 41.1 | 1862 | 3705 | 1501 | 7069 |
| **Subtotal** | **60 764** | **19.3** | **50.4** | **30.3** | **69.9** | **37.8** | **18.2** | **23 115** | **38.0** | **3534** | **19 047** | **15 068** | **37 649** |
| **Total** | **170 737** | **19.2** | **49.1** | **31.7** | **35.0** | **23.9** | **10.1** | **36 980** | **21.7** | **21 287** | **63 770** | **48 700** | **133 757** |

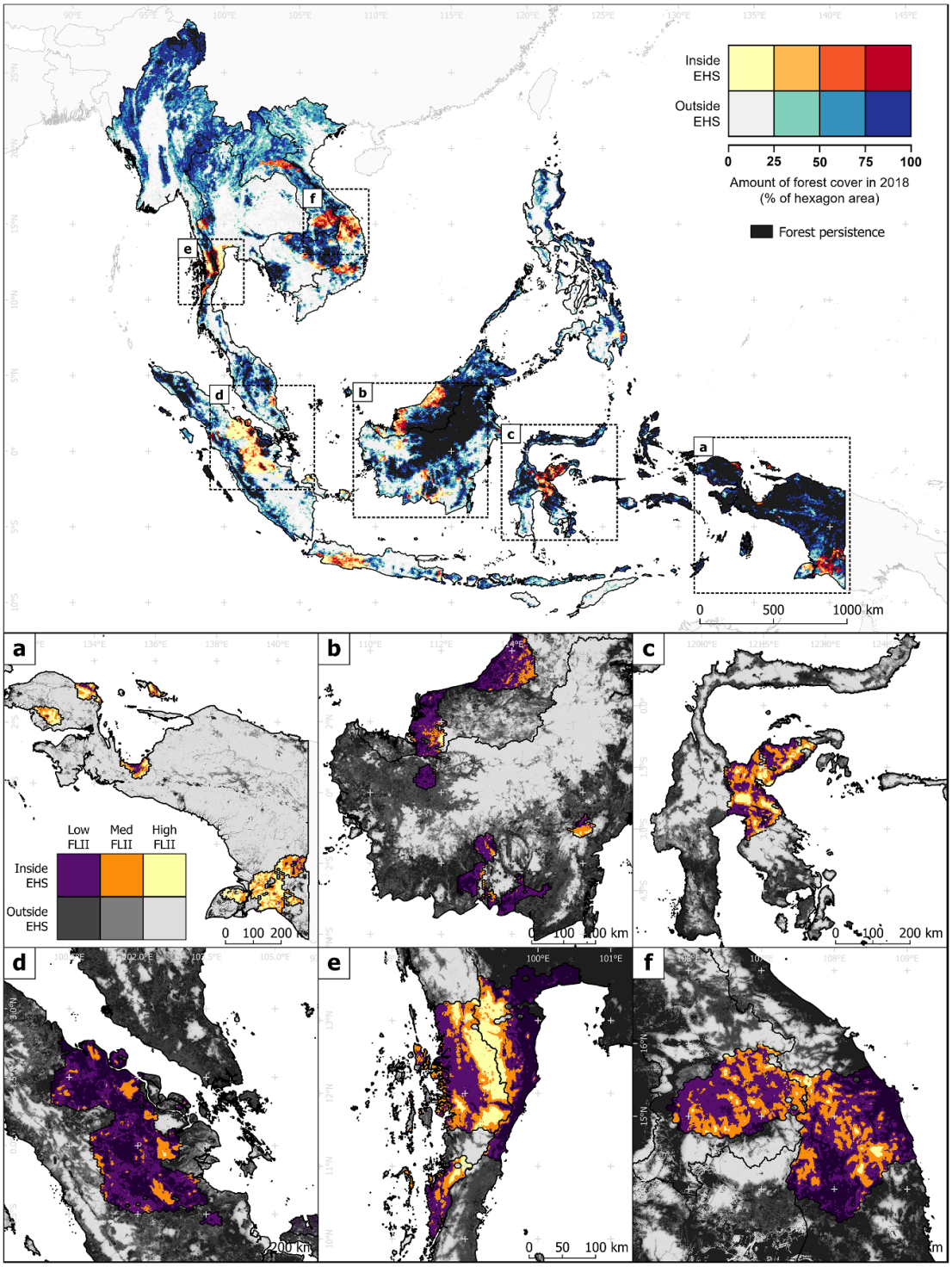


**Figure 5.** State of SE Asia's remaining forest in emergent hot spots (EHS). Regional map (top) showing the amount of remaining 2018 ESA forest that occur inside and outside EHS, where each map unit is a 5 km circumradius hexagon (~65 km$^2$). Insets show the distribution of high, med (medium), and low integrity forest using the 2019 Forest Landscape Integrity Index (FLII) data for hot spots in (a) Papua, (b) Borneo, (c) Sulawesi, (d) Sumatra, (e) Tenasserim, and (f) southern Laos and central Vietnam.

## 4. Discussion

Oil palm and rubber plantations were the predominant drivers of EHS deforestation in SE Asia, corroborating a large literature on their contributions to deforestation in the region (Ziegler *et al* 2009, Gunarso *et al* 2013, Abood *et al* 2015, Gaveau *et al* 2016, Hurni and Fox 2018). We found, further, that oil palm-related deforestation in the Sumatra and Sarawak EHS has been on the decline since 2012, but expansion has shifted to Papua and Kalimantan, a trend in line with the suggestion that oil palm expansion is being displaced to new forest frontiers to meet rising global demand (Kongsager and Reenberg 2012, Pirker *et al* 2016, Vijay *et al* 2016, Austin *et al* 2017). Given that recent palm oil production volumes

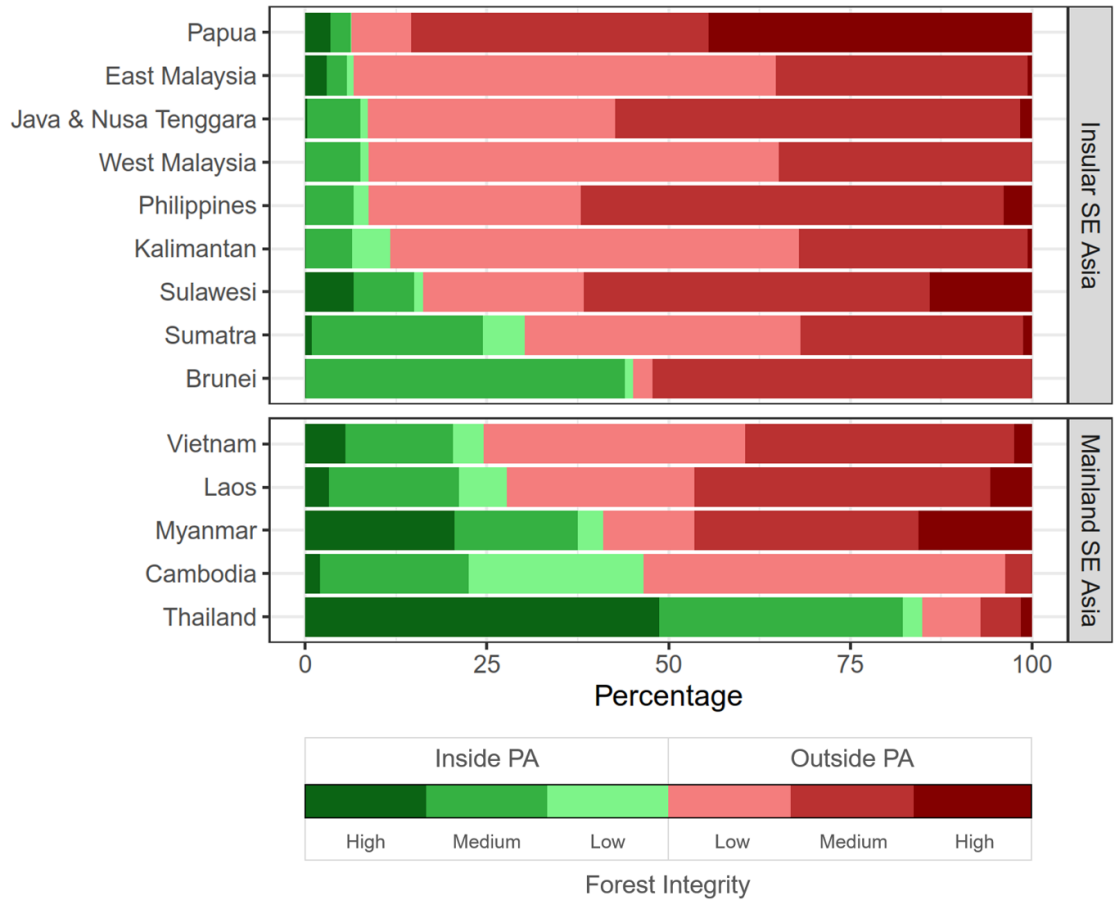


**Figure 6.** Integrity of protected and unprotected forest in emergent hot spots (EHS), as of 2019. Stacked bars depict the percentage contribution of high, medium, and low-integrity forest inside and outside protected areas (PA), within EHS.

and futures are increasing (FAOSTAT 2021, USDA-FAS 2021), there is an emergent threat of oil-palm driven deforestation in SE Asia, especially in the Papuan frontier that presently remains largely intact. Heightened protection is thus needed to effectively mitigate against the loss of such forests, but these could be coupled with alternative strategies to develop oil palm on underutilized or degraded land (Goh *et al* 2018), or with appropriate oversight and enforcement pursuant to strict certification standards such as No Deforestation, No Peat, No Exploitation commitments (European Palm Oil Alliance 2021).

In the case of rubber plantations in mainland SE Asia, we show that rubber-driven deforestation was prominent in EHS of Tanintharyi and Cambodia, particularly after 2006 when rubber prices were increasing (figure S8). Given that there is a demonstrable link between rubber prices and deforestation (Grogan *et al* 2019), and that rubber is typically considered a long-term investment that smallholder farmers—who form the bulk of rubber production (Fox and Castella 2013)—are reluctant to convert, it is plausible that rubber will remain a major driver of deforestation, particularly when prices trend upward, as has been the case since early 2019 (figure S8). Based on our analysis, we expect future expansion to occur in EHS along the Tenasserim and Annamite mountain ranges, thus supporting previous studies that forewarned of rubber expansion towards marginal environments and higher elevations (Ahrends *et al* 2015, Zeng *et al* 2018). Considering that these regions still possess substantial forest cover, a resurgence of rubber-driven deforestation would present a double threat of habitat loss and localized warming (Zeng *et al* 2020) that would increasingly threaten biodiversity.

Our analyses revealed shifting cultivation as a minor driver of EHS deforestation, which contrasts with narratives identifying it as the primary cause of widespread deforestation across SE Asia (see Fox 2000, Fox *et al* 2009). Where swidden occurred, we found that a majority were converted to tree plantations and mixed farming systems, reflecting the regionwide transition of traditional swidden to more permanent and intensified forms of agricultural production (Vongvisouk *et al* 2014, Suhardiman *et al* 2019). The low importance of shifting cultivation as a deforestation driver in this study may in part be because swidden fields tend to have a small individual footprint (i.e. smaller than an ESA 9-ha pixel), and do not characteristically exhibit spatiotemporal clustering.

Of all remaining forest in SE Asia, 9.0% were found in EHS; these are the areas most actively threatened with habitat loss, indicating a need for conservation prioritization. However, only 35.0% of high-integrity and 23.9% of medium-integrity EHS forest is protected; these values are lower than the global averages reported by Grantham *et al* (2020), where 52.3% of high-integrity and 30.3% of medium-integrity forest are protected globally. Our results further demonstrate that this shortfall in existing protection of high and medium integrity forests is severely pronounced in EHS of insular SE Asia, where only ∼15% of both high and medium-integrity forest are presently protected, which contrasts starkly with EHS of mainland SE Asia where 69.9% of high-integrity and 37.8% of medium-integrity forest are protected. These findings therefore suggest—solely from a standpoint of spatial coverage—that the current protected area network is likely to be insufficiently poised to deal with frontier deforestation in the region, especially in insular SE Asia.

Despite only comprising 19% of all threatened forest, high-integrity forest should be prioritized due to their unrivalled importance in the provision of multifarious ecosystem services (Grantham *et al* 2020). Indeed, their loss represents a keystone environmental problem in that it would trigger disproportionately large and long-term consequences that could offset decades of conservation progress and climate action, particularly in areas containing vulnerable, yet irreplaceable carbon stocks (Noon *et al* 2021). By contrast, medium-integrity forest, which contribute substantially to ecosystem function—albeit at reduced levels due to their semi-disturbed state (Grantham *et al* 2020)—constituted 49% of all threatened EHS forest. Therefore, conservation prioritization must carefully balance the trade-offs in securing safeguards for invaluable, yet less extensive high-integrity forest, versus administering immediate interventions for more expansive, yet relatively less protected medium-integrity forest. These findings underscore the importance of systematic conservation planning (Maxwell *et al* 2020, De Alban *et al* 2021) to address emergent deforestation in the region, especially in highly contested forest frontiers where we anticipate tree-plantation expansion to continue driving deforestation.

## 5. Significance of Emergent Threat Analysis

Emergent Threat Analysis supports proactive conservation strategies through the integration of Emerging Hot Spot Analysis, visual classification of deforestation outcomes over time, and spatial quantification of contemporary forest condition and protection to identify increasingly threatened, high value forested landscapes. Individually, each method provides useful geospatial information on land cover and change; however, Harris *et al* (2017) noted the opportunity to combine metrics of forest loss clustering with contextual information, and Emergent Threat Analysis integrates and synergizes those information flows. Importantly, the underlying data sets are replaceable according to research needs and data availability. For example, the identification of EHS would remain effective with other forest loss datasets (e.g. Harris *et al* 2017, Pacheco *et al* 2021). Further, we use VHR imagery to visually discriminate between deforestation outcomes over time, but this could be substituted with increasingly finer scale imagery (e.g. Planet Team 2017), or augmented with automated classification techniques. Similarly, whereas we used the FLII because it delivered the most contemporary data relevant to the long-term preservation of forest connectivity and ecosystem function (Grantham *et al* 2020), other geospatial databases relating to the present state, quality, and/or value of extant forest could be used. Given this flexibility, Emergent Threat Analysis is highly relevant to a diverse set of stakeholders ranging from conservation scientists, practitioners, legislators, lobbyists, and donors, who, in congruence with the 2030 global sustainability agenda, share cooperative interests in targeting deforestation fronts across the global tropics (Pacheco *et al* 2021).

## Data availability statement

All data that support the findings of this study are included within the article (and any supplementary files). The raw geospatial data can be obtained from the following sources: ESA annual land cover maps (https://maps.elie.ucl.ac.be/CCI/viewer/), Global Administrative Areas version 3.4 (https://gadm.org/download_country.html), 2019 Forest Landscape Integrity Index (www.forestlandscapeintegrity.com/download-data), and protected areas (www.protectedplanet.net/en (version July 2021), and Wildlife Conservation Society Myanmar).

## Acknowledgment

This research was supported by Singapore Ministry of Education Academic Research Grant Tier 1 to E L W. Open access funded by Helsinki University Library.

## Author contributions

Conceptualization: J J, J D T D A, and E L W; methodology: J J; analysis: J J and E L W; interpretation of results: J J, J D T D A, L R C, and E L W; writing: J J and E L W; review and editing: J D T D A and L R C; supervision: E L W; funding: L R C and E L W.

## Conflict of interest

The authors declare no competing interest.

## ORCID iDs

Johanness Jamaludin https://orcid.org/0000-0001-7043-4814
Jose Don T De Alban https://orcid.org/0000-0002-1671-5786
L Roman Carrasco https://orcid.org/0000-0002-2894-1473
Edward L Webb https://orcid.org/0000-0001-5554-9955

## References

Abood S A, Lee J S H, Burivalova Z, Garcia-Ulloa J and Koh L P 2015 Relative contributions of the logging, fiber, oil palm, and mining industries to forest loss in Indonesia *Conserv. Lett.* **8** 58–67

Achard F *et al* 2014 Determination of tropical deforestation rates and related carbon losses from 1990 to 2010 *Glob. Change Biol.* **20** 2540–54

Ahrends A, Hollingsworth P M, Ziegler A D, Fox J M, Chen H, Su Y and Xu J 2015 Current trends of rubber plantation expansion may threaten biodiversity and livelihoods *Glob. Environ. Change* **34** 48–58

ArcGIS 2021 How Emerging Hot Spot Analysis works—ArcGIS Pro|documentation (available at: https://pro.arcgis.com/en/pro-app/latest/tool-reference/space-time-pattern-mining/learnmoreemerging.htm)

Austin K G, Mosnier A, Pirker J, McCallum I, Fritz S and Kasibhatla P S 2017 Shifting patterns of oil palm driven deforestation in Indonesia and implications for zero-deforestation commitments *Land Use Policy* **69** 41–48

Baccini A *et al* 2012 Estimated carbon dioxide emissions from tropical deforestation improved by carbon-density maps *Nat. Clim. Change* **2** 182–5

Bey A *et al* 2016 Collect Earth: land use and land cover assessment through augmented visual interpretation *Remote Sens.* **8** 807

Bivand R, Ono H, Dunlap R, Stigler M, Denney B and Hernangómez D 2020 *classInt*: choose univariate class intervals (available at: https://CRAN.R-project.org/package=classInt)

Brodzik M, Billingsley B, Haran T, Raup B and Savoie M 2012 EASE-Grid 2.0: incremental but significant improvements for Earth-gridded data sets *Int. J. Geo-Inf.* **1** 32–45

Bürgi M, Hersperger A M and Schneeberger N 2005 Driving forces of landscape change—current and new directions *Landsc. Ecol.* **19** 857–68

Curtis P G, Slay C M, Harris N L, Tyukavina A and Hansen M C 2018 Classifying drivers of global forest loss *Science* **361** 1108–11

De Alban J D T, Jamaludin J, de Wen D W, Than M M and Webb E L 2020 Improved estimates of mangrove cover and change reveal catastrophic deforestation in Myanmar *Environ. Res. Lett.* **15** 034034

De Alban J D T, Leong B P I, Venegas-Li R, Connette G M, Jamaludin J, Latt K T, Oswald P, Reeder C and Webb E L 2021 Conservation beyond the existing protected area network is required to improve species and habitat representation in a global biodiversity hotspot *Biol. Conserv.* **257** 109105

De Alban J D T, Prescott G W, Woods K M, Jamaludin J, Latt K T, Lim C L, Maung A C and Webb E L 2019 Integrating analytical frameworks to investigate land-cover regime shifts in dynamic landscapes *Sustainability* **11** 1139

Dinerstein E *et al* 2017 An ecoregion-based approach to protecting half the terrestrial realm *BioScience* **67** 534–45

Dudley N and Phillips A 2006 Forests and protected areas: guidance on the use of the IUCN protected area management categories IUCN (available at: https://portals.iucn.org/library/node/8804)

ESA 2017 *ESA. Land Cover CCI Product User Guide Version 2. Tech. Rep.* (available at: www.esa-landcover-cci.org/?q=webfm_send/84)

European Palm Oil Alliance 2021 NDPE: no deforestation, peat and exploitation *European Palm Oil Alliance* (available at: https://palmoilalliance.eu/ndpe-commitment/)

FAOSTAT 2021 FAOSTAT (available at: www.fao.org/faostat/en/#data)

Feng Y, Ziegler A D, Elsen P R, Liu Y, He X, Spracklen D V, Holden J, Jiang X, Zheng C and Zeng Z 2021 Upward expansion and acceleration of forest clearance in the mountains of Southeast Asia *Nat. Sustain.* **4** 892–9

Finer M, Novoa S, Weisse M J, Petersen R, Mascaro J, Souto T, Stearns F and Martinez R G 2018 Combating deforestation: from satellite to intervention *Science* **360** 1303–5

Fox J 2000 How blaming 'slash and burn' farmers is deforesting mainland Southeast Asia (available at: http://scholarspace.manoa.hawaii.edu/handle/10125/3832)

Fox J and Castella J-C 2013 Expansion of rubber (*Hevea brasiliensis*) in Mainland Southeast Asia: what are the prospects for smallholders? *J. Peasant Stud.* **40** 155–70

Fox J, Fujita Y, Ngidang D, Peluso N, Potter L, Sakuntaladewi N, Sturgeon J and Thomas D 2009 Policies, political-economy, and swidden in Southeast Asia *Hum. Ecol.* **37** 305–22

Gaveau D L A, Sheil D, Husnayaen S M A, Arjasakusuma S, Ancrenaz M, Pacheco P and Meijaard E 2016 Rapid conversions and avoided deforestation: examining four decades of industrial plantation expansion in Borneo *Sci. Rep.* **6** 32017

Geist H J and Lambin E F 2002 Proximate causes and underlying driving forces of tropical deforestation *BioScience* **52** 143

Getis A and Ord J K 1992 The analysis of spatial association by use of distance statistics *Geogr. Anal.* **24** 189–206

Giam X 2017 Global Biodiversity Loss from Tropical Deforestation *PNAS* **114** 5775–7

Gibbs H K and Herold M 2007 Tropical deforestation and greenhouse gas emissions *Environ. Res. Lett.* **2** 045021

Goh C S, Junginger M, Potter L, Faaij A and Wicke B 2018 Identifying key factors for mobilising under-utilised low carbon land resources: a case study on Kalimantan *Land Use Policy* **70** 198–211

Grantham H S *et al* 2020 Anthropogenic modification of forests means only 40% of remaining forests have high ecosystem integrity *Nat. Commun.* **11** 5978

Grogan K, Pflugmacher D, Hostert P, Mertz O and Fensholt R 2019 Unravelling the link between global rubber price and tropical deforestation in Cambodia *Nat. Plants* **5** 47–53

Gunarso P, Hartoyo M E, Agus F and Killeen T J 2013 Roundtable on Sustainable Palm Oil *Oil Palm and Land Use Change in Indonesia, Malaysia and Papua New Guinea* p 36

Hansen M C *et al* 2013 High-resolution global maps of 21st-century forest cover change *Science* **342** 850–3

Hansen M C, Krylov A, Tyukavina A, Potapov P V, Turubanova S, Zutta B, Ifo S, Margono B, Stolle F and Moore R 2016 Humid tropical forest disturbance alerts using Landsat data *Environ. Res. Lett.* **11** 034008

Hansen M C, Stehman S V and Potapov P V 2010 Quantification of global gross forest cover loss *Proc. Natl Acad. Sci.* **107** 8650–5

Harris N L *et al* 2017 Using spatial statistics to identify emerging hot spots of forest loss *Environ. Res. Lett.* **12** 024012

Hersperger A M, Gennaio M-P, Verburg P H and Bürgi M 2010 Linking land change with driving forces and actors: four conceptual models *Ecol. Soc.* **15**

Hesselbarth M H K, Sciaini M, With K A, Wiegand K and Nowosad J 2019 Landscapemetrics: an open-source R tool to calculate landscape metrics *Ecography* **42** 1648–57

Hijmans R J *et al* 2021 *raster*: geographic data analysis and modeling (available at: https://CRAN.R-project.org/package=raster)
Hoang N T and Kanemoto K 2021 Mapping the deforestation footprint of nations reveals growing threat to tropical forests *Nat. Ecol. Evol.* **5** 845–53
Hosonuma N, Herold M, de Sy V, de Fries R S, Brockhaus M, Verchot L, Angelsen A and Romijn E 2012 An assessment of deforestation and forest degradation drivers in developing countries *Environ. Res. Lett.* **7** 044009
Hughes A C 2017 Understanding the drivers of Southeast Asian biodiversity loss *Ecosphere* **8** e01624 10.1002/ecs2.1624
Hurni K and Fox J 2018 The expansion of tree-based boom crops in mainland Southeast Asia: 2001–2014 *J. Land Use Sci.* **13** 198–219
IUCN, UNEP-WCMC 2020 *The World Database on Protected Areas (WDPA)* (Cambridge: United Nations Environment Programme World Conservation Monitoring Centre)
IUCN, UNEP, and WCMC 2021 *The Restoration Initiative: 2020 Year in Review* (Rome: IUCN, FAO, UNEP)
Jayathilake H M, Prescott G W, Carrasco L R, Rao M and Symes W S 2020 Drivers of deforestation and degradation for 28 tropical conservation landscapes *Ambio* **50** 215–28
Kendall M G and Gibbons J D 1990 *Rank Correlation Methods* 5th edn (New York: Oxford University Press) p 272
Kenney-Lazar M and Ishikawa N 2019 Mega-plantations in Southeast Asia: landscapes of displacement *Environ. Soc.: Adv. Res.* **10** 63–82
Kongsager R and Reenberg A 2012 *Contemporary land-use transitions: The global oil palm expansion* 4 Global Land Project
Lawrence D and Vandecar K 2015 Effects of tropical deforestation on climate and agriculture *Nat. Clim. Change* **5** 27–36
Lepers E, Lambin E F, Janetos A C, DeFries R, Achard F, Ramankutty N and Scholes R J 2005 A synthesis of information on rapid land-cover change for the period 1981–2000 *BioScience* **55** 115
Lim C L, Prescott G W, De Alban J D T, Ziegler A D and Webb E L 2017 Untangling the proximate causes and underlying drivers of deforestation and forest degradation in Myanmar *Conserv. Biol.* **31** 1362–72
Mann H B 1945 Nonparametric tests against trend *Econometrica* **13** 245–59
Margono B A, Potapov P V, Turubanova S, Stolle F and Hansen M C 2014 Primary forest cover loss in Indonesia over 2000–2012 *Nat. Clim. Change* **4** 730–5
Mather A S 1992 The forest transition *Area* **24** 367–79
Maxwell S L *et al* 2020 Area-based conservation in the 21st century *Nature* **586** 217–27
Miettinen J, Shi C and Liew S C 2011 Deforestation rates in insular Southeast Asia between 2000 and 2010 *Glob. Change Biol.* **17** 2261–70
Mitchard E T A 2018 The tropical forest carbon cycle and climate change *Nature* **559** 527–34
Mousivand A and Arsanjani J J 2019 Insights on the historical and emerging global land cover changes: the case of ESA-CCI-LC datasets *Appl. Geogr.* **106** 82–92
Myers N, Mittermeier R A, Mittermeier C G, da Fonseca G A B and Kent J 2000 Biodiversity hotspots for conservation priorities *Nature* **403** 853–8
Noon M L *et al* 2021 Mapping the irrecoverable carbon in Earth's ecosystems *Nat. Sustain.* **5** 37–46
Nowosad J, Stepinski T F and Netzel P 2019 Global assessment and mapping of changes in mesoscale landscapes: 1992–2015 *Int. J. Appl. Earth Obs. Geoinf.* **78** 332–40
NYDF Assessment Partners 2021 *Progress on the New York Declaration on Forests: Taking Stock of Climate Change Action for Forests. Goal 7 Progress Report* (available at: https://forestdeclaration.org/resources/taking-stock-of-national-climate-action-for-forests/)
Pacheco P, Mo K, Dudley N, Shapiro A, Aguilar-Amuchastegui N, Ling P Y, Anderson C and Marx A 2021 Deforestation fronts: drivers and responses in a changing world (WWF International) (available at: https://wwf.panda.org/discover/our_focus/forests_practice/deforestation_fronts_/)
Pebesma E *et al* 2021 *sf*: simple features for R (available at: https://CRAN.R-project.org/package=sf)
Pirker J, Mosnier A, Kraxner F, Havlík P and Obersteiner M 2016 What are the limits to oil palm expansion? *Glob. Environ. Change* **40** 73–81
Planet Team 2017 *Planet Application Program Interface: In Space for Life on Earth* (San Francisco, CA: Planet Labs PBC)
Prescott G W *et al* 2017 Political transition and emergent forest-conservation issues in Myanmar *Conserv. Biol.* **31** 1257–70
QGIS Development Team 2021 Quantum GIS homepage (available at: https://qgis.org/en/site/)
R Core Team 2020 R: a language and environment for statistical computing (Vienna: R Foundation for Statistical Computing) (available at: www.r-project.org/)
Ramankutty N and Coomes O 2016 Land-use regime shifts: an analytical framework and agenda for future land-use research *Ecol. Soc.* **21**
Reiche J *et al* 2021 Forest disturbance alerts for the Congo Basin using Sentinel-1 *Environ. Res. Lett.* **16** 024005
Richards D R and Friess D A 2016 Rates and drivers of mangrove deforestation in Southeast Asia, 2000–2012 *Proc. Natl Acad. Sci. USA* **113** 344–9
Rudel T K, Defries R, Asner G P and Laurance W F 2009 Changing drivers of deforestation and new opportunities for conservation *Conserv. Biol.* **23** 1396–405
Schepaschenko D *et al* 2019 Recent advances in forest observation with visual interpretation of very high-resolution imagery *Surv. Geophys.* **40** 839–62
Sodhi N S, Koh L P, Brook B W and Ng P K L 2004 Southeast Asian biodiversity: an impending disaster *Trends Ecol. Evol.* **19** 654–60
Stibig H-J, Achard F, Carboni S, Raši R and Miettinen J 2014 Change in tropical forest cover of Southeast Asia from 1990 to 2010 *Biogeosciences* **11** 247–58
Suhardiman D, Keovilignavong O and Kenney-Lazar M 2019 The territorial politics of land use planning in Laos *Land Use Policy* **83** 346–56
UNEP-WCMC 2015 *World Database on Protected Areas User Manual 1.1* (Cambridge: UNEP-WCMC)
USDA-FAS 2021 Oilseeds: World Markets and Trade (available at: https://usda.library.cornell.edu/concern/publications/tx31qh68h?locale=en)
Verma A, Schmidt-Vogt D, De Alban J D T, Lim C L and Webb E L 2021 Drivers and mechanisms of forest change in the Himalayas *Glob. Environ. Change* **68** 102244
Vijay V, Pimm S L, Jenkins C N and Smith S J 2016 The impacts of oil palm on recent deforestation and biodiversity loss *PLoS One* **11** e0159668
Vongvisouk T, Mertz O, Thongmanivong S, Heinimann A and Phanvilay K 2014 Shifting cultivation stability and change: contrasting pathways of land use and livelihood change in Laos *Appl. Geogr.* **46** 1–10
Wickham H 2021 tidyr: tidy messy data (available at: https://CRAN.R-project.org/package=tidyr)
Wickham H, Chang W, Henry L, Pedersen T L, Takahashi K, Wilke C, Woo K, Yutani H, Dunnington D and RStudio 2021a *ggplot2*: create elegant data visualisations using the grammar of graphics (available at: https://CRAN.R-project.org/package=ggplot2)
Wickham H, François R, Henry L and Müller K (RStudio) 2021b *dplyr*: a grammar of data manipulation (available at: https://CRAN.R-project.org/package=dplyr)
Zeng Y, Maxwell S, Runting R K, Venter O, Watson J E M and Carrasco L R 2020 Environmental destruction not avoided with the sustainable development goals *Nat. Sustain.* **3** 795–8
Zeng Z, Estes L, Ziegler A D, Chen A, Searchinger T, Hua F, Guan K, Jintrawet A and Wood F E 2018 Highland cropland expansion and forest loss in Southeast Asia in the twenty-first century *Nat. Geosci.* **11** 556–62
Ziegler A D, Fox J M and Xu J 2009 The rubber juggernaut *Science* **324** 1024–5